

ARTICLE

Linear and Nonlinear Optical Properties of Novel Multi-branched Oligomers

Li-jing Gong^{a,c}, Ying-hui Wang^{a*}, Zhi-hui Kang^a, Tian-hao Huang^a, Ran Lu^b, Han-zhuang Zhang^{a*}*a. College of Physics, Jilin University, Changchun 130012, China**b. College of Chemistry, Jilin University, Changchun 130012, China**c. Aviation University of Air Force, Changchun 130022, China*

(Dated: Received on October 19, 2012; Accepted on November 27, 2012)

We investigate the fluorene-vinylene unit dependent photo-physical properties of multi-branched truxene based oligomers (Tr-OFV_n, $n=1-4$) employing steady-state absorption and emission spectroscopy, transient absorption spectroscopy, two-photon fluorescence, and z-scan technique. The results show that the increasing of fluorene-vinylene unit leads to a red-shift in the spectra of absorption and fluorescence, and shortens the excited state lifetime. Meanwhile, two-photon fluorescence efficiency and two-photon absorption cross section of truxene based oligomers gradually enhance in company with the extension of π -conjugated length. In addition, the values of two-photon absorption cross section modeled on the sum-over-state approach agree well with the experimental ones. The results indicate multi-branched truxene based oligomers bearing oligo(fluorene-vinylene) arms are promising organic materials for two-photon applications.

Key words: Multi-branch oligomer, Two-photo absorption, Z-scan

I. INTRODUCTION

The multi-branched oligomers acting as one of the important oligomers, have attracted much attention due to their excellent two-photon optical properties [1, 2]. In this type of process, two photons are absorbed simultaneously, exciting the oligomers to a higher energy state with the energy increase being equal to the sum of the photon energies. This characteristic provides a wide range of applications, such as photodynamic therapy [3–5], optical storage [6], optical limiting [7–9], 3D micro-fabrication [10, 11], and two-photon fluorescence microscopy [12] *etc.* The organic molecule with two-photon optical property has developed significantly over the past twenty years [13, 14]. People gradually realize that the two-photon optical property of organic materials depends on the donor-acceptor strength, molecular structure and conjugation length, *etc.* [15]. Based on symmetrical (D- π -D or A- π -A, D, A, and π are electron donor, acceptor, and π -electron bridge, respectively) or asymmetrical (D- π -A) structures, many types of π -conjugated units were chose, such as pyrene, benzene, biphenyl, fluorene, dithienothiophene, and dihydrophenanthrene [16, 17] moieties, and a large number of organic molecules with strong nonlinear photo-physical properties were synthesized [18, 19]. Recently, Lu *et al.* have reported a series of novel multi-branched mono-disperse conjugated truxene based oligomers bearing oligo(fluorene-vinylene) arms (Tr-OFV_n ($n=1-4$)) [20].

Fluorene-vinylene group acts as a π -conjugated unit and π -electron bridge, and has excellent property of electron delocalization. The side chains were also introduced to improve the solubility of oligomer. These multi-branched oligomers exhibit strong two-photon absorption (TPA) cross-section [20], even though they have no strong donor and acceptor units. However, thus so far, reports that focus on conjugated system without strong donor and acceptor units are limited, it is necessary to better understand their basic optical properties and photo-physical mechanism.

In this work, we investigate fluorene-vinylene (FV) unit dependent photo-physical properties of these novel multi-branched oligomers (Tr-OFV_n ($n=1-4$)) (as seen in Fig.1) in detail, employing steady-state absorption and emission spectroscopy, transient absorption spectroscopy, two-photon fluorescence (TPF) and z-scan technique, and finally model the value of TPA cross-section by using the sum-over-state (SOS) approach with a five-energy-level system. The results offer a broadband analysis of structure-property relationship and show that the π -conjugated extension leads to a red-shift in absorption and emission spectra, and shortens the excited state lifetime and finally improves the two-photon optical properties of oligomers. The study gives a better understanding about the factors for good two-photon optical properties of this kind of oligomers.

II. EXPERIMENTS

Toluene solutions of Tr-OFV_n ($n=1-4$) with concentrations of 0.025 and 0.5 mmol/L are prepared for linear and nonlinear optical measurements, respectively. The

* Authors to whom correspondence should be addressed. E-mail: zhanghz@jlu.edu.cn, yinghui_wang@jlu.edu.cn

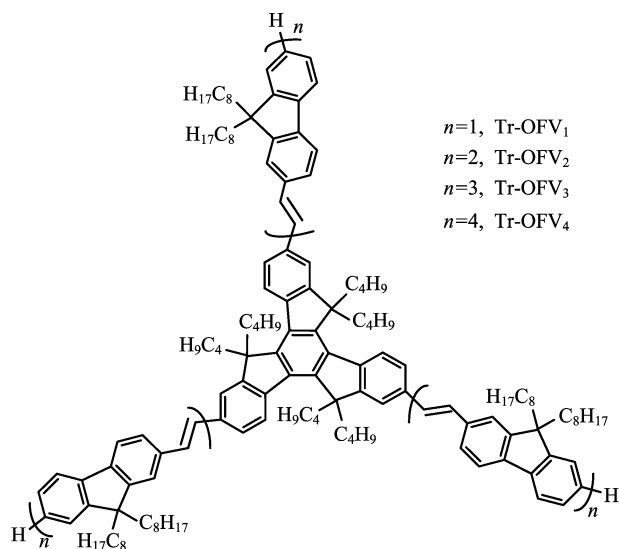


FIG. 1 Molecular structure of Tr-OFV_n ($n=1-4$).

samples were placed in a 2 mm thick quartz cuvette to perform the optical measurements. Femtosecond Titanium:Sapphire laser (Coherent) was used as radiation source, which offered 2.2 mJ, 130 fs pulses at 800 nm with a repetition rate of 1 kHz.

Steady-state absorption spectra were obtained using a UV-Vis absorption spectrometer (Purkinje, TU-1810PC) and steady-state fluorescence spectra were measured by CCD detector (Ocean Optics, USB4000). The TPA property was investigated via the open-aperture z-scan technique with femtosecond laser pulse, which was modulated by a mechanical chopper (~ 500 Hz) and then refocused with a lens onto a PMT (Zolix, PMTH-S1-CR131A). The TPA cross-section $\sigma^{(2)}$ can be obtained through the expression

$$\sigma^{(2)} = \frac{h\nu\beta}{N} \quad (1)$$

where N is the number of molecules per cm^3 , β is the nonlinear absorption coefficient, and $h\nu$ is the photon energy. $\sigma^{(2)}$ is expressed in Göppert-Mayer units ($1 \text{ GM} = 10^{-50} \text{ (cm}^4 \text{ s) / (molecule photon)}$).

In the transient absorption measurement, the output beam of the femtosecond laser was split into two parts. One part focused into a 5 mm quartz cell filled with water to generate a white light continuum as the probe beam, and the other part was sent to a 1 mm thick BBO crystal to generate the double frequency of 400 nm excitation pulses as the pump beam to excite the sample, which was modulated by a mechanical chopper (~ 500 Hz). Both of pump and probe beam focused into the sample cuvette and overlapped with each other. The time-dependent change of the transmittance passed through the mono-chromator, and was detected by PMT (Zolix, PMTH-S1-CR131A). The relative polarization of the excitation and the probe beams

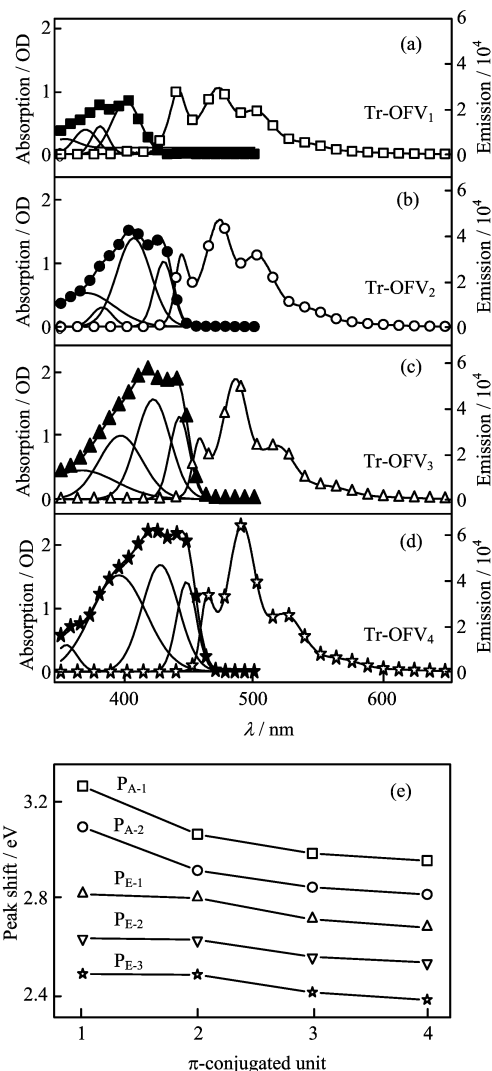


FIG. 2 (a)–(d) Spectra of steady-state absorption (solid symbol) and OPF (open symbol) of Tr-OFV_n ($n=1-4$) with concentration of 0.025 mmol/L, and (e) the variation of spectral feature with the increasing of π -conjugated units. The solid lines in absorption spectra represent the fitting Gaussian line-shape on the basis of the steady absorption spectra and offer the spectroscopic parameters to use in the sum-over-state approach.

were set to the magic angle for all the measurements. All electronic signals which traveled through the lock-in amplifier from PMT were able to obviously suppress noise outside a narrow frequency interval, before they reach the computer. The excitation spot was $\sim 500 \mu\text{m}$ in diameter. The energy of probe beam was < 0.1 nJ, while the pump beam was around ~ 1.5 nJ. All experiments were performed at room temperature.

III. RESULTS AND DISCUSSION

The absorption and fluorescence spectra of Tr-OFV_n ($n=1-4$) in toluene (0.025 mmol/L) are shown in Fig.2

TABLE I The photo-physical parameters obtained in experimental and theoretical data.

	Stokes shift/cm ⁻¹	ESL/ns	ψ_n/ψ_1	$\beta/(10^{-3} \text{ cm/GW})$	$\sigma_E^{(2)a}/10^3 \text{ GM}$	$\sigma_T^{(2)b}/10^3 \text{ GM}$
Tr-OFV ₁	3791	1.09	1	14.5	1.20	0.96
Tr-OFV ₂	3544	1.00	4	21.0	1.73	2.18
Tr-OFV ₃	3426	0.89	9	27.5	2.27	2.45
Tr-OFV ₄	3370	0.73	18	41.5	3.43	3.33

^a $\sigma_E^{(2)}$: the experimental values of TPA cross-section, employing z-scan technique.

^b $\sigma_T^{(2)}$: the theoretical calculated values of TPA cross-section by using SOS approach.

(a)–(d). Being transparent in the near infrared region, all multi-branch conjugated truxene derivatives (Tr-OFV_{*n*} (*n*=1–4)) show a subtle structure in the spectra of absorption and one-photon fluorescence (OPF). Taking Tr-OFV₁ as an example, it shows two obvious absorption features and a shoulder in absorption spectra, which are at 3.09, 3.26, and 3.43 eV, respectively, and three clear emission peaks at 2.82, 2.64, and 2.48 eV. The first absorption peak of Tr-OFV₁ at 3.09 eV in the red region of absorption spectra should be mainly assigned to the S₀→S₁ transition and the second around 3.26 eV, which is much closed to the first absorption peak, may be attributed to S₀→S₂ transition. According to the molecular structure, we could speculate that these oligomers all own C₃ symmetry, therefore the transition of S₀→S₂ should be dipole forbidden. However, the absorption spectra of oligomers aren't consistent with our speculation, such as that of Tr-OFV₁, indicating that the transition of S₀→S₂ becomes partially allowed upon relaxation of the molecular geometry to a conformation with lower symmetry. The subtle spectral features in the absorption and OPF spectra both exhibit a red-shift behavior with the increasing of FV unit as shown in Fig.2(e), and accompany with an enhancement in the absorption coefficients and fluorescence efficiency.

In addition, these subtle spectral features are still seen in THF solution [16], indicating that the mechanism of transition and emission is almost independent of the solvent polarity. We also calculate the Stokes shift of Tr-OFV_{*n*} (*n*=1–4) in toluene according to their normalized absorption and OPF spectra (Table I). Apparently, the Stokes shift decreases from 3791 cm⁻¹ to 3370 cm⁻¹ when the number of FV unit increases from 1 to 4. Meanwhile, we measured the excited state lifetimes for all oligomers using femtosecond transient absorption technique. Figure 3 shows the kinetic traces probed at 860 nm for Tr-OFV_{*n*} (*n*=1–4) in toluene solution (0.5 mmol/L), which is described by a mono-exponential decay function. The fitting results are summarized in Table I. Apparently, when FV unit increases from 1 to 4, the excited state lifetime gradually shortens from 1.09 ns to 0.73 ns, indicating that the π -conjugated extension is able to facilitate the relaxation of isolated excited oligomers.

Under the excitation of 800 nm femtosecond pulses,

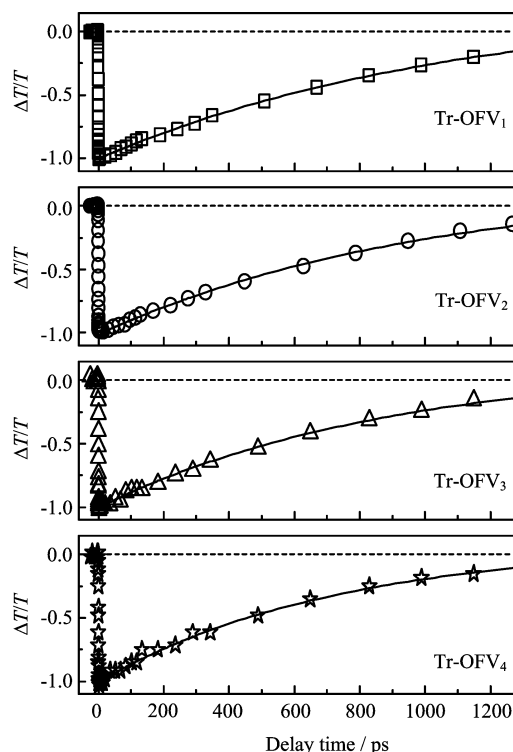


FIG. 3 Transient absorption traces at 860 nm of Tr-OFV_{*n*} (*n*=1–4) with excitation pulse at 400 nm. The excited state lifetimes (ESL) were determined through the mono-exponential function and summarized in Table I.

Tr-OFV_{*n*} (*n*=1–4) in toluene solution (0.5 mmol/L) emits intense photoluminescence (PL) and the normalized emission spectra are shown in Fig.4(a). We measure the PL spectra under different excitation light intensities, and the integral PL intensities have a characteristic dependence on the square of the excitation light intensity (Fig.4(b)). Combined with steady-state absorption spectra, it provides reliable evidence that the fluorescence excited by 800 nm laser pulse originates from the TPA process and follows the equation [21]:

$$I_{\text{TPF}} = S\delta\psi I_{800}^2 \quad (2)$$

$$\psi = \sigma^{(2)}\varphi^{(2)}N \quad (3)$$

where *S* is the intensity of the signal collected by a

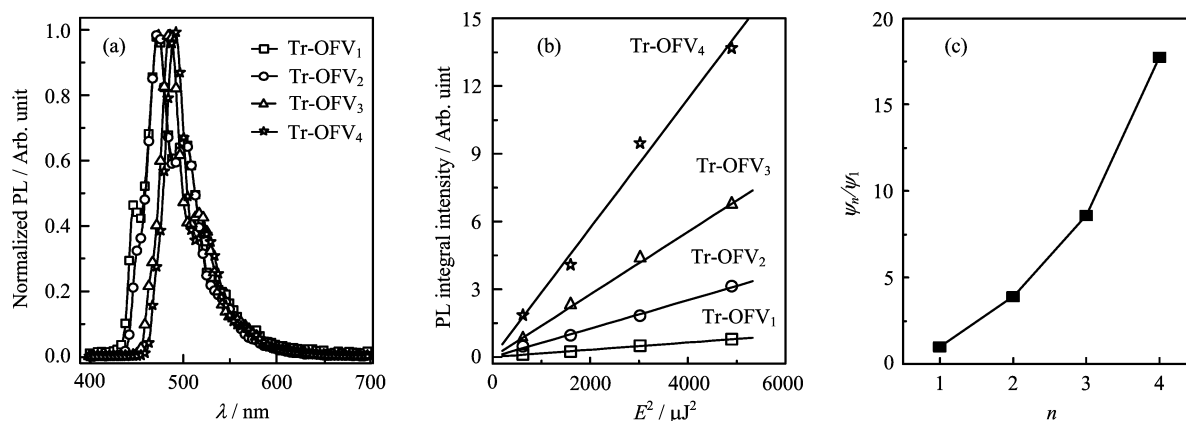


FIG. 4 (a) Normalized PL spectra of Tr-OFV_n ($n=1-4$) excited by 800 nm femtosecond pulse, (b) the PL integral intensities of Tr-OFV_n ($n=1-4$) as a function of the square of the laser energy E^2 , and (c) the π -conjugated unit dependence of ψ_n/ψ_1 ($n=1-4$).

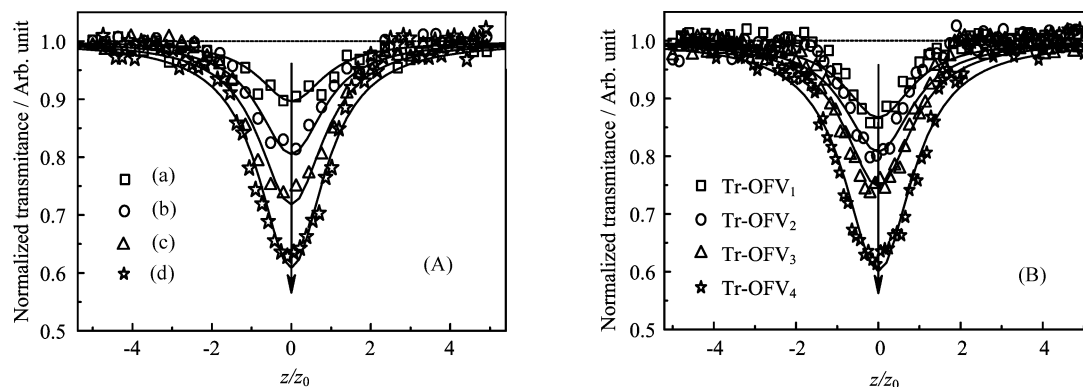


FIG. 5 (A) Intensity dependent open-aperture z-scan profiles for Tr-OFV₄, (a)–(d) pulse energies are 65, 125, 185, and 245 nJ, respectively, β values in (a)–(d) are 42.0×10^{-3} , 42.5×10^{-3} , 41.5×10^{-3} , and 42.5×10^{-3} cm/GW, respectively. (B) Open-aperture z-scan signatures for Tr-OFV_n ($n=1-4$) (energy of pulse: ~ 245 nJ). The solid lines represent fitting lines used to extract β value.

CCD detector, δ is the overall fluorescence collection efficiency of the experimental apparatus, ψ is TPF efficiency of sample, $\varphi^{(2)}$ is the TPF quantum yield. In comparison with OPF spectra, the positions of the first emission peaks in TPF spectra are all red-shifted ~ 30 meV, as seen in Fig.4(a). The relative amplitude of the first emission peak compared to the total fluorescence spectra weakens apparently, which could be explained by the re-absorption effect, because of the solutions with a much higher concentration (0.5 mmol/L). Figure 4(c) shows the evolution of ψ_n/ψ_1 with the increase of the FV unit, showing that the TPF efficiency ψ of Tr-OFV_n ($n=2-4$) increases to 4, 9, and 18 times in comparison with that of Tr-OFV₁, indicating that improvement of TPF efficiency profits from enhancing the ICT character, due to the extension of π -conjugated system.

In order to further ascertain the relationship between oligomer structure and the TPF efficiency, we use femtosecond open-aperture z-scan technique to measure the TPA cross-section of Tr-OFV_n ($n=1-4$). Firstly,

we conducted the open-aperture z-scan experiments on neat toluene with the pulse energy of 245 nJ, and the results show that there is no effect of the laser beams on the 2 mm quartz cell containing the solvent. Therefore, we could exclude the influence of the solvent non-linearity. The z-scan signatures of Tr-OFV₄ recorded with different incident pulse energies exhibit a minimum near the beam waist as shown in Fig.5(A), which can be contributed to the nonlinear absorption process. The nonlinear absorption coefficient β can be measured by fitting the experimental data with equation [22]:

$$T(z, S = 1) = \sum_{m=0}^{\infty} \frac{[-q_0(z, 0)]^m}{(m+1)^{3/2}} \quad (4)$$

$$q_0(z) = \frac{\beta I_0}{1 + z^2/z_0^2} \quad (5)$$

where T is the normalized transmittance for the open-aperture z-scan curve, $z_0 = k\omega_0^2/2$ is the Rayleigh length, $k = 2\pi/\lambda$ is the wave vector, ω_0 is beam waist radius of Gaussian pulse, I_0 is the pulse irradiance.

TABLE II Spectroscopic parameters used in the SOS approach, employing the five-energy-level system.

	ν_{10}	ν_{20}	ν_{30}	ν_{40}	Γ_{10}^a	Γ_{20}	Γ_{30}	Γ_{40}	μ_{10}/D	μ_{20}/D	μ_{30}/D	μ_{40}/D
Tr-OFV ₁	24955	26307	27119	28325	1837	825	1243	1362	12.8	5.3	4.4	4.5
Tr-OFV ₂	23272	24617	26196	27119	663	1359	933	2756	10.6	6.6	4.0	3.6
Tr-OFV ₃	22640	23730	25245	27356	640	1272	1831	3448	11.7	6.1	5.1	4.2
Tr-OFV ₄	22363	23435	25340	28268	650	1306	2899	1155	12.5	5.0	9.0	2.5

^a Γ (in cm^{-1}) is the damping constant describing the full width at half-maximum of the final state line-width, and $\nu_{m0} = \omega_{m0}/2\pi$ (ν_{m0} is in unit of cm^{-1}).

The open-aperture z-scan traces of Tr-OFV₄ recorded with different incident pulse energies exhibit similar z-scan curves, and the corresponding β is about $41.5 \times 10^{-3} \text{ cm/GW}$ and almost independent of femtosecond pulse energy, indicating that the observed nonlinear absorption is originated from TPA. If higher-order absorption, such as the simultaneous three-photon absorption, is involved in the observation [23], the value of β could obviously deviate upward from $41.5 \times 10^{-3} \text{ cm/GW}$ at the high incident power and show incident power dependent enhancement behavior. Figure 5(b) shows open-aperture femtosecond z-scan measurements for Tr-OFV_{*n*} ($n=1-4$) in toluene solution (0.5 mmol/L). The experimental values of the TPA cross-section ($\sigma_E^{(2)}$) are summarized in Table I. When the pulse energy is about 245 nJ, the change of transmission at waist gradually enhances with the increasing of FV unit, showing that $\sigma_E^{(2)}$ becomes larger on account for the extending of π -conjugation. When the FV unit increases from 1 to 4, the TPA cross-section is not able to enhance 4 times. Therefore, extension of π -conjugated system could improve the TPA property, the amplitude of enhancement is limited in a certain extent.

To further understand the results, we use SOS model to calculate the TPA cross section $\sigma_T^{(2)}$, where TPA cross-section depends on two factors: transition dipole moments and transition frequencies of the molecules. As all oligomers studied here belong to the same family of compounds, we assume that these truxene derivatives Tr-OFV_{*n*} ($n=1-4$) all have five states, one initial ground state (0), one intermediate state (1), and three final states (2, 3, and 4), and the TPA cross-section can be written as [24]:

$$\sigma^{(2)} = \frac{4}{5\pi} \frac{(2\pi)^4}{(ch)^2} \frac{\nu_p^2}{(\nu_{10} - \nu_p)^2 + \Gamma_{10}^2} \cdot \left[\frac{|\mu_{21}|^2 |\mu_{10}|^2 \Gamma_{20}}{(\nu_{20} - 2\nu_p)^2 + \Gamma_{20}^2} + \frac{|\mu_{31}|^2 |\mu_{10}|^2 \Gamma_{30}}{(\nu_{30} - 2\nu_p)^2 + \Gamma_{30}^2} + \frac{|\mu_{41}|^2 |\mu_{10}|^2 \Gamma_{40}}{(\nu_{40} - 2\nu_p)^2 + \Gamma_{40}^2} \right] \quad (6)$$

where c and h are the speed of light and the Planck constant, respectively, ν_{m0} ($m=1-4$) is the transition frequency of the $0 \rightarrow m$ transition, Γ is a damping con-

stant related to the intermediate states, ν_p is the laser frequency, $\vec{\mu}_{m0}$ ($m=1-4$) is transition moment vector ($|\vec{\mu}_{m1}| = |\vec{\mu}_{m0} - \vec{\mu}_{10}|$, $m=1-4$). And $\vec{\mu}_{m0}$ ($m=1-4$) can be calculated as follows [25]:

$$|\vec{\mu}_{m0}| = \sqrt{\frac{3}{4\pi} \frac{c}{\pi^{1/2}} \sigma_{m0}^{\max} \frac{\Gamma_{m0}}{2(\ln 2)^{1/2}} \frac{h}{\nu_{m0}}} \quad (7)$$

σ_{m0}^{\max} is the Gaussian fitting peak value of m state. Most of the spectroscopic parameters used in this model (SOS) can be obtained from the linear absorption spectra, such as the transition frequency and damping factor. In this way, we fit the linear absorption spectra shown in Fig.2, assuming that the absorption bands of the compounds investigated exhibit a Gaussian line-shape given by the following [25]:

$$g_{m0}(\omega) = 2\sqrt{\frac{\ln 2}{\pi}} \frac{A_{m0}}{\Gamma_{m0}} \exp \left[-4 \ln 2 \left(\frac{\omega_{m0} - \omega}{\Gamma_{m0}} \right)^2 \right] \quad (8)$$

where A_{m0} is the amplitude of Gaussian line-shape, Γ_{m0} is the full width at half-maximum of Gaussian line-shape, showing the damping constant of the m state, ω_{m0} is the center frequency of Gaussian line-shape, describing the transition frequency between m state and ground state. Table II summarizes the spectroscopic parameters used in the SOS approach in order to model the theoretical value of $\sigma_T^{(2)}$. However, according to the absorption spectra of oligomers, the spectral feature of S₁ state shows that its band edge in red region is steep and its peak is also narrow, so the width of fitted Gaussian peak, which corresponds to the S₁ state in the absorption spectra, is narrower in comparison with that of emission spectra. In this way, a rough approximation for the $\sigma_T^{(2)}$ values can be obtained from the Eq.(6), which are summarized in Table I. So we can see that the theoretical values of $\sigma_T^{(2)}$ are much closed to the experimental values $\sigma_E^{(2)}$ and show the enhancement behavior accompanied with the increasing of FV unit. Apparently, our theoretical and experimental results are consistent with the molecular design strategy, which is based on the concept that with increasing the oligomer conjugated length, and the $\sigma^{(2)}$ can be improved through enhancing the ICT character.

IV. CONCLUSION

We reported the π -conjugated unit dependent optical properties of truxene based oligomers bearing oligo(fluorene-vinylene) arms. The linear spectral measurement shows that the π -conjugated extension leads to the red-shift in absorption and fluorescence spectra, and accelerates the relaxation of isolated excited oligomers. The nonlinear optical measurement exhibits that extension of the conjugation length is useful for improving the TPA cross-section and TPF quantum yield. Meanwhile, the theoretical SOS calculation of the TPA cross-sections of Tr-OFV_n ($n=1-4$) studied here are in good agreement with the experimental value obtained from z-scan technique. From a technological point of view, the results open the door to access a new family of materials with excellent two-photon optical properties.

V. ACKNOWLEDGMENTS

This work was supported by the National Natural Science Foundation of China (No.10774060, No.10974071, No.21103161, and No.11274142), the Jilin Province Natural Science Foundation of China (No.20070512), the National Undergraduate Innovation Foundation of China (No.2011A32045), the National Foundation for Fostering Talents of Basic Science (No.J1103202), and the China Postdoctoral Science Foundation (No.2011M500927).

- [1] C. Andraud, R. Fortrie, C. Barsu, O. Stephan, H. Chermette, and P. L. Baldeck, *Adv. Polym. Sci.* **214**, 149 (2008).
- [2] T. Francesca, K. Claudine, B. Ekaterina, T. Sergei, and B. D. Mireille, *Adv. Mater.* **20**, 4641 (2008).
- [3] D. Gao, R. R. Agayan, H. Xu, M. A. Philbert, and R. Kopelman, *Nano Lett.* **6**, 2383 (2006).
- [4] W. R. Dichtel, J. M. Serin, C. Edder, J. M. J. Fréchet, M. Matuszewski, L. S. Tan, T. Y. Ohulchanskyy, and P. N. Prasad, *J. Am. Chem. Soc.* **126**, 5380 (2004).
- [5] M. Atif, P. E. Dyer, T. A. Paget, H. V. Snelling, and M. R. Stringer, *Photodiag. Photodyn. Ther.* **4**, 106 (2007).
- [6] D. A. Parthenopoulos and P. M. Rentzepis, *Science* **245**, 843 (1989).
- [7] I. Fuks-Janczarek, J. Ebothe, R. Miedzinski, R. Gabanski, A. H. Reshak, M. Lapkowski, R. Motyka, I. V. Kityk, and J. Suwinski, *Laser Phys.* **18**, 1056 (2008).
- [8] M. P. Joshi, H. E. Pudavar, J. Swiatkiewicz, P. N. Prasad, and B. A. Reinhardt, *Appl. Phys. Lett.* **74**, 170 (1999).
- [9] H. B. Sun, T. Suwa, K. Takada, R. P. Zaccaria, M. S. Kim, K. S. Lee, and S. Kawata, *Appl. Phys. Lett.* **83**, 1104 (2004).
- [10] S. Kawata, H. B. Sun, T. Tanaka, and K. Takada, *Nature* **412**, 697 (2001).
- [11] W. Zhou, S. M. Kuebler, K. L. Braun, T. Yu, J. K. Cammack, C. K. Ober, J. W. Perry, and S. R. Marder, *Science* **296**, 1106 (2002).
- [12] M. C. Skala, J. M. Squirrel, K. M. Vrotsos, V. C. Eickhoff, A. Gendron-Fitzpatrick, K. W. Eliceiri, and N. Ramanujam, *Cancer Res.* **65**, 1180 (2005).
- [13] S. R. Marder, D. N. Beratan, and L. T. Cheng, *Science* **252**, 103 (1991).
- [14] D. R. Kanis, M. A. Ratner, and T. J. Marks, *Chem. Rev.* **94**, 195 (1994).
- [15] D. Beljonne, W. Wenseleers, E. Zojer, Z. Shuai, H. Vogel, S. J. K. Pond, J. W. Perry, S. R. Marder, and J. L. Bredas, *Adv. Funct. Mater.* **12**, 631 (2002).
- [16] M. H. V. Werts, S. Gmouh, O. Mongin, T. Pons, and M. Blanchard-Desce, *J. Am. Chem. Soc.* **126**, 16294 (2004).
- [17] H. Detert, M. Lehmann, and H. Meier, *Materials* **3**, 3218 (2010).
- [18] J. E. Ehrlich, X. L. Wu, I. Y. S. Lee, Z. Y. Hu, H. Röckel, S. R. Marder, and J. W. Perry, *Opt. Lett.* **22**, 1843 (1997).
- [19] O. K. Kim, K. W. Lee, H. Y. Woo, K. S. Kim, G. S. He, J. Swiatkiewicz, and P. N. Prasad, *Chem. Mater.* **12**, 284 (2000).
- [20] H. P. Zhou, X. Zhao, T. H. Huang, R. Lu, H. Z. Zhang, X. H. Qi, P. C. Xue, X. L. Liu, and X. F. Zhang, *Org. Biomol. Chem.* **9**, 1600 (2011).
- [21] J. Yoo, S. K. Yang, M. Y. Jeong, H. C. Ahn, S. J. Jeon, and B. R. Cho, *Org. Lett.* **5**, 645 (2003).
- [22] M. Sheik-Bahae, A. A. Said, T. H. Wei, D. J. Hagan, and E. W. Van Stryland, *IEEE J. Quantum Electron.* **26**, 760 (1990).
- [23] S. V. Rao, T. S. Prashant, D. Swain, T. Sarma, P. K. Panda, and S. P. Tewari, *Chem. Phys. Lett.* **514**, 98 (2011).
- [24] K. Kamada, K. Ohta, I. Yoichiro, and K. Kondo, *Chem. Phys. Lett.* **372**, 386 (2003).
- [25] M. G. Vivas, S. L. Nogueira, H. Santos Silva, N. M. Barbosa Neto, A. Marletta, F. Serein-Spirau, S. Lois, T. Jarrosson, L. De Boni, R. A. Silva, and C. R. Mendonca, *J. Phys. Chem. B* **115**, 12687 (2011).